Nuclear Instruments and Methods in Physics Research B 382 (2016) 71–75

Contents lists available at ScienceDirect

Nuclear Instruments and Methods in Physics Research B

journal homepage: www.elsevier.com/locate/nimb

Irradiation of graphene field effect transistors with highly charged ions

P. Ernst *, R. Kozubek, L. Madauß, J. Sonntag, A. Lorke, M. Schleberger

Fakultät für Physik and CENIDE, Universität Duisburg-Essen, 47048 Duisburg, Germany

ARTICLE INFO

Article history:
Received 19 January 2016
Accepted 17 March 2016
Available online 27 April 2016

Keywords:
Graphene
Highly charged ion
Field-effect transistor
Transfer characteristic
Raman measurement

ABSTRACT

In this work, graphene field-effect transistors are used to detect defects due to irradiation with slow, highly charged ions. In order to avoid contamination effects, a dedicated ultra-high vacuum set up has been designed and installed for the in situ cleaning and electrical characterization of graphene field-effect transistors during irradiation. To investigate the electrical and structural modifications of irradiated graphene field-effect transistors, their transfer characteristics as well as the corresponding Raman spectra are analyzed as a function of ion fluence for two different charge states. The irradiation experiments show a decreasing mobility with increasing fluences. The mobility reduction scales with the potential energy of the ions. In comparison to Raman spectroscopy, the transport properties of graphene show an extremely high sensitivity with respect to ion irradiation: a significant drop of the mobility is observed already at fluences below 15 ions/μm^2, which is more than one order of magnitude lower than what is required for Raman spectroscopy.

1. Introduction

The irradiation with energetic ions may be used to obtain permanent modifications of surfaces [1–6,5,7–11] or so-called 2D materials such as graphene, carbon nanomembranes, MoS_2, and hexagonal BN [4,12–19]. For 2D materials in particular, slow highly charged ion (HCI) beams seem to be the appropriate tool as these projectiles deposit their potential energy, i.e. the sum of the ionization energies of the missing electrons, in a very small volume close to the surface. However, despite ongoing research in this field [1,20,2,21,17], the underlying interaction mechanisms are still not very well understood, in particular with respect to 2D materials. In the case of HCI it is rather difficult to distinguish between the influence of the key parameters, i.e. the kinetic energy E_{kin} and the potential energy E_{pot}, as a complete deceleration of the ions is not feasible [22]. One method is to keep one parameter fixed and vary the other to find a threshold value for a given modification. With respect to graphene, such a threshold has already been determined by atomic force microscopy (AFM) [17], while this has yet to be done with Raman spectroscopy. Both methods are very powerful tools to investigate irradiation effects in graphene but have their disadvantages as well. The AFM may detect individual impact sites on the order of one per μm^2, provided they are large enough. Raman spectroscopy on the other hand is sensitive to the smallest defects [23–25], but is only effective at relatively high fluences, starting from 10^{10} ions/cm^2 (corresponding to 100 ions/μm^2) onwards. In addition, most experiments are performed ex situ under ambient conditions, i.e. the samples have to be taken out of the irradiation chamber and as a consequence undergo additional, uncontrolled changes. In this paper we present an alternative method to estimate ion-induced radiation damage, which is sensitive in a fluence regime that bridges the two aforementioned methods. We use field-effect transistors (FET) made from single layer graphene [26,27]. We show that by analyzing the transfer characteristics of graphene FETs (G-FETs) before and after irradiation, conclusions with respect to ion-induced defects in graphene may be drawn.

2. Experiment

2.1. Experiment

For this experiment, single layer graphene was mechanically exfoliated onto oxidized (285 nm SiO_2), degenerately p-doped Si wafers. Metallic contacts were provided by photolithography and vacuum evaporation of a 5 nm thick Ti adhesion layer and a 100 nm thick gold layer. The graphene quality is checked by μ-Raman spectroscopy (ReniShaw, $\lambda = 532$ nm, $P = 1$ mW) before and after photolithography, and after irradiation as well (see Section 3.1). Fig. 1 shows a schematic sketch of our devices with the typical channel length and width of $L = 5$ μm and $W = 5$ μm, respectively. In this configuration, the degenerately doped Si works as a global backgate (U_{GS}), whereas the gold contacts are used as

* Corresponding author.
E-mail address: marika.schleberger@uni-due.de (M. Schleberger).

http://dx.doi.org/10.1016/j.nimb.2016.03.043
0168-583X/

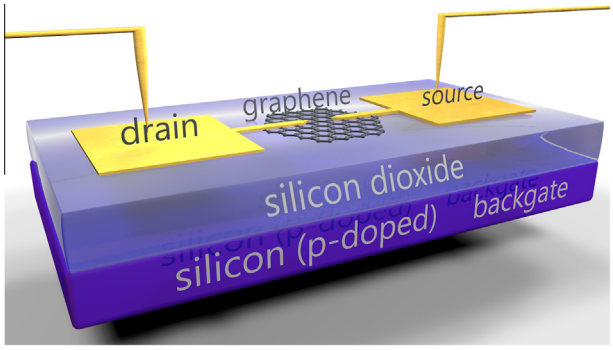

Fig. 1. Schematic sketch of a graphene field-effect transistor (G-FET).

both the drain and the source contact. The transfer characteristic $I_{DS}(U_{GS})$ reflecting the electrical properties of the G-FETs is measured before, during and after irradiation with HCIs. The current I_{DS} between drain and source is driven by a constant potential difference U_{DS}. In order to calculate the electron and hole mobility, respectively, the following equation can be used [28]

$$\mu_{\pm} = \sigma \frac{L}{WC_i U_{DS}}. \quad (1)$$

The differential conductance is given by $\sigma = \frac{\partial I_{DS}}{\partial U_{GS}}$ and the sheet capacitance $C_i = \frac{\epsilon_0 \epsilon}{d} = 1.212 \cdot 10^{-8}$ F/cm^2, with $\epsilon = 3.9$ [28] being the dielectric constant of SiO_2 with a thickness of $d = 285$ nm. Additionally, the charge carrier density can be calculated by [29]

$$n = \frac{C_i}{e}(U_{Dirac} - U_{GS}) \quad (2)$$

where e is the elementary charge and U_{Dirac} is the voltage, at which the Dirac point (characterized by $n \approx p \approx 0$, i.e. minimum conductivity) is observed.

In order to be able to measure the transfer characteristic during irradiation with HCI, a dedicated ultra high vacuum (UHV) set up for the G-FETs was built. To this end, the G-FETs were bonded onto a custom-made, UHV compatible chip carrier. Furthermore, the G-FETs were cleaned by heating at around $T = 150$ °C before irradiation to partly remove intercalated water and residual photoresist (see Section 4.1) stemming from the preparation procedure [30,31]. All samples were irradiated using the Duisburg HCI beamline HICS [32], which is based on an electron beam ion trap (EBIT) that can produce ^{129}Xe ions with a charge state q from 1+ to 45+ and a corresponding maximum potential energy of about e.g. $E_{pot} = 58.8\ keV$. The kinetic energy $E_{kin} = q(U_{acc} - U_{dec})$ can be controlled via a deceleration stage and is given by the charge state of the ion q, the acceleration voltage U_{acc}, and the deceleration voltage U_{dec}. The charge state selection is done with a dipole magnet, whereas a multi-stage lens system ensures a focused ion beam with a spot size of less than 1 mm^2 diameter. A Faraday-Cup is used to measure the beam current.

In previous experiments, the threshold charge state for ion-induced modifications of graphene was found to be $^{129}Xe^{30+}$ (corresponding to a potential energy of $E_{pot} \approx 15$ keV) at a kinetic energy of $E_{kin} \approx 260$ keV [17]. Therefore, we have chosen two charge states, one below and one above this threshold, namely $^{129}Xe^{25+}$ ($E_{pot} \approx 8$ keV) and $^{129}Xe^{32+}$ ($E_{pot} \approx 19$ keV), while keeping the kinetic energy fixed at $E_{kin} \approx 200$ keV. For both charge states, the transfer characteristic is measured as a function of the ion fluence in the range of 0 to about 2500 ions/cm^2. The back-gate-voltage is varied from $U_{GSmin} = -20$ V to $U_{GSmax} = +20$ V, while the drain-source-voltage is held constant at $U_{DS} = 50$ mV for all measurements.

3. Results

3.1. Raman-spectra

Raman spectroscopy can be used as a non-destructive method to analyze the structural quality of graphene and in particular, the existence, density and type of defects [33–36]. A typical Raman spectrum of exfoliated, high-quality graphene shows two prominent peaks [24,25]: The in-plane vibrational G mode at $\approx$1580 cm^{-1} and the $2D$ mode at $\approx$2690 cm^{-1}. The full width at half maximum (FWHM) of the 2D peak can be used to determine the layer thickness. A FWHM $\approx$ 25 cm^{-1} indicates single layer graphene, whereas a FWHM $\approx$ 52 cm^{-1} is typically found for bilayer graphene [37]. The $2D$ mode is sometimes also called the second-order in-plane overtone of the D mode vibration. The presence of the first order D mode at $\approx$ 1350 cm^{-1} is indicative for lattice defects or disorder, respectively [38]. The D mode as well as the D' mode at $\approx$1620 cm^{-1} can be used for defect analysis [39,33,34]. In Fig. 2 Raman spectra from our samples are shown, the first taken from pristine graphene (black line), the second from graphene after photolithography (blue line), and finally from irradiated graphene (red line). The FWHM of the $2D$ mode of pristine graphene (black line) is about $\approx$ 27 cm^{-1} and thus indicates single layer graphene. The absence of the D-Peak (black line) proves the high quality of the graphene flakes after exfoliation [40].

For a quantitative comparison of irradiation-induced disorder, we analyze the area ratios of the D and G mode, A_D/A_G [41,33]. Already due to the photolithography process (blue line) this ratio typically increases up to $A_D/A_G = 0.3$. After irradiation with $^{129}Xe^{32+}$ ions (>2500 ions/μm^2), an area ratio of $A_D/A_G = 3.5$ is measured (red line). Note, that in order to guarantee a sufficient signal/noise ratio of the relevant Raman peaks, graphene has to be irradiated with a fluence of at least 100–500 ions/μm^2, depending on the charge state.

4. Electrical characterization before irradiation

Without cleaning, the G-FETs fabricated as described above, are typically p-doped [26]. This becomes apparent in the transfer characteristic $I_{DS}(U_{GS})$ measurements, shown in Fig. 3a, where the Dirac-point is shifted to a high, positive backgate voltage. After the cleaning process, which consists of heating the sample in

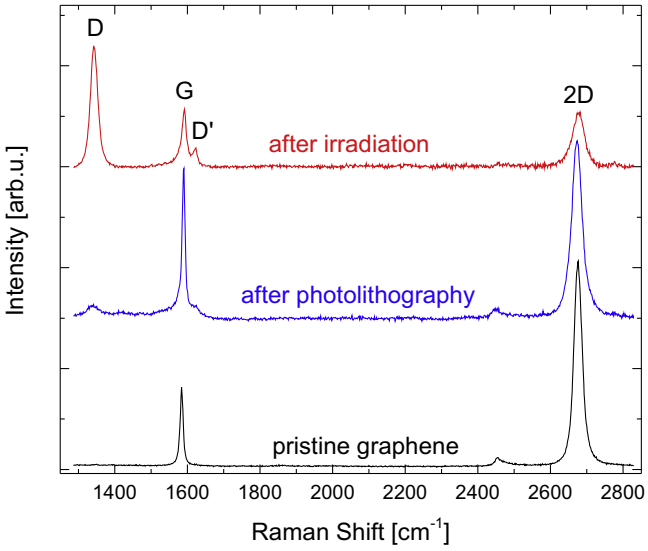

Fig. 2. Typical Raman-spectra from pristine graphene (black line), after photolithography (blue line) and after irradiation with HCIs (red Line). The different Raman modes are marked. (For interpretation of the references to colour in this figure legend, the reader is referred to the web version of this article.)

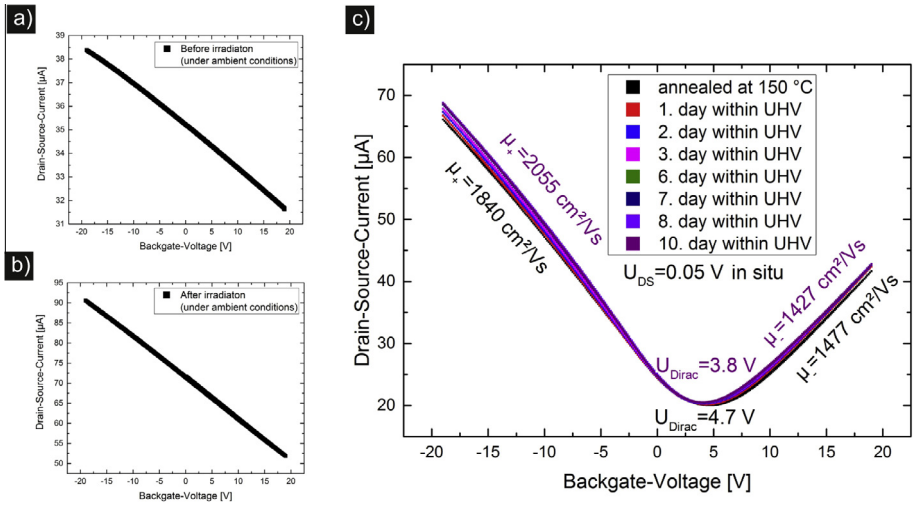

Fig. 3. A typical transfer characteristic under ambient condition before (a) and after irradiation (b) shows a well p-doped G-FET. The transfer characteristic curves vary only very slightly for the G-FET after annealing at 150 °C and stored for 10 days within the UHV chamber (c).

UHV at 150 °C for 24 h, the Dirac-point typically lies between $U_{GSmin} = -20$ V and $U_{GSmax} = +20$ V. Because of the limited thermal stability of the chip carrier, the temperatures used here are slightly lower compared to published values [30,31]. The heating time can be used to achieve a given doping level and Dirac-point position in a wide range [42], e.g. the initially *p*-doped G-FET may become non-doped with a Dirac-Point close to $U_{GS} = 0$ V, or even *n*-doped for longer heating times. For an analysis of relative changes due to ion irradiation, the absolute value of the Dirac point is not so important, but the stability of the Dirac point, as well as a stable charge carrier mobility $\mu_{\pm}$ of non-irradiated devices, are of course crucial. To test this, we have prepared a G-FET with a Dirac-Point close to $U_{GS} = 0$ V and stored it inside the UHV chamber for several days (base pressure $p = 5 \cdot 10^{-9}$ mbar). In Fig. 3c one can see that the transfer characteristic curves vary only very slightly. After taking the G-FET out of the UHV, it returned to its inital *p*-doped state which is typical for exposure to ambient conditions (see Fig. 3b).

Note that the transfer characteristics shown in Fig.3 are typical for G-FETs, but the absolute values for individual G-FETs may vary significantly. In order to eliminate this uncontrollable variation of the initial values and still be able to compare ion-induced effects in G-FETs with different initial transfer characteristics, we use relative values instead. For example, the last measurement before irradiation (purple line in Fig. 3c) is used to calculate the reference mobilities of this G-FET: $\mu_{reference+} = 2055\ \frac{cm^2}{Vs}$ and $\mu_{reference-} = 1427\ \frac{cm^2}{Vs}$. After the reference values have been determined from the cleaned G-FET, the relative charge carrier mobility after irradiation is given by:

$$\mu_{rel} = \frac{\mu_{after}}{\mu_{reference}} \tag{3}$$

This means that any effect of HCI irradiation on the charge carrier mobilities is measured with respect to the data measured just before irradiation. This procedure is valid as in between individual irradiation steps, the FET is not taken out of the UHV. In this way the individual quality of a given G-FETs is factored out and even non-ideal G-FETs with below average mobility values can be used for the experiment.

4.1. Electrical characterization after irradiation

After irradiation with highly charged ions, the G-FETs typically show a reduction of both, electron and hole mobility. Fig. 4a shows the relative electron (red) and hole (black) mobility during irradiation with $^{129}Xe^{32+}$ and Fig. 4b for irradiation with $^{129}Xe^{25+}$. From the data it can be clearly seen that the reduction of mobility scales with the potential energy of the ions. At the same fluence, e.g. about 1000 ions/µm^2, the relative electron and hole mobility after $^{129}Xe^{32+}$-irradiation ($^{32+}\mu_{relative,+} = 0.29$) is significantly smaller than after irradiation with $^{129}Xe^{25+}$ ($^{25+}\mu_{relative,+} = 0.55$). Another remarkable result is the extreme sensitivity of the G-FET: The mobility is already affected at fluences <15 ions/µm^2. Additionally, the residual charge carrier density (blue) is plotted as a function of the ion fluence in Fig. 4. Obviously, the ongoing irradiation with HCI leads to an increasing hole density (initial state of the G-FETs: $^{129}Xe^{32+}$-irradiation *p*-doped with $n = 2.9 \cdot 10^{11}$ cm^{-2} and $^{129}Xe^{32+}$-irradiation *n*-doped with $n = -4 \cdot 10^{11}$ cm^{-2}).

4.2. Annealing after irradiation

Finally, we annealed (2 h at 110 °C) the G-FETs after irradiation to test if we could recover the initial state. From Fig. 5 one can see that the hole mobility stays nearly constant at $\mu_{+} = 198\ \frac{cm^2}{Vs}$ and that the only significant change is the shift of the Dirac-Point to lower backgate voltages from $U_{GS} = 12.75$ V to $U_{GS} = 4.375$ V. This indicates that the ion irradiation causes structural damage to the graphene lattice, which cannot be cured by moderate thermal annealing.

5. Discussion

Our data shows that G-FETs can indeed be used for the investigation of HCI-induced defects in graphene. In addition, G-FETs are much more sensitive than Raman spectroscopy. The transport properties are already affected at fluences on the order of 10 ions/µm^2, which is the domain of spatially resolved methods such as AFM. A detailed analysis of the relation between defect structure and electronic transport properties seems thus feasible with G-FETs. The processing of our devices already gives rise to a certain number of defects which can be seen from the Raman data. This might represent a drawback, as the graphene is no longer pristine when exposed to the ion beam. On the other hand, the devices are stable in UHV and can be controlled in a reproducible way by in situ heating with respect to the initial doping level. Thus, we could show that the observed effects during irradiation are exclusively related to the irradiation and not to other transient effects.

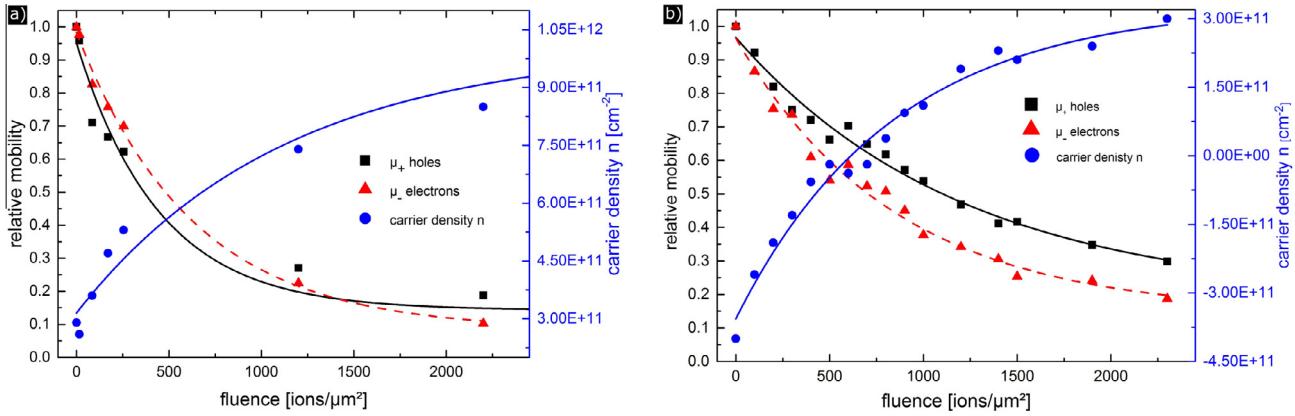

Fig. 4. The relative mobility for holes (black) and electrons (red) as well as the carrier density (blue, right scale) is plotted against the fluence of bombarded $^{129}Xe^{32+}$-ions, whereas solid lines are a guide to the eye. The relative electron and hole mobility after $^{129}Xe^{32+}$-irradiation (a) is significantly smaller than after irradiation with $^{129}Xe^{25+}$ (b). It is also remarkable, that the influence of highly charged ions is already measurable at low fluences (<15 ions/µm^2). (For interpretation of the references to colour in this figure legend, the reader is referred to the web version of this article.)

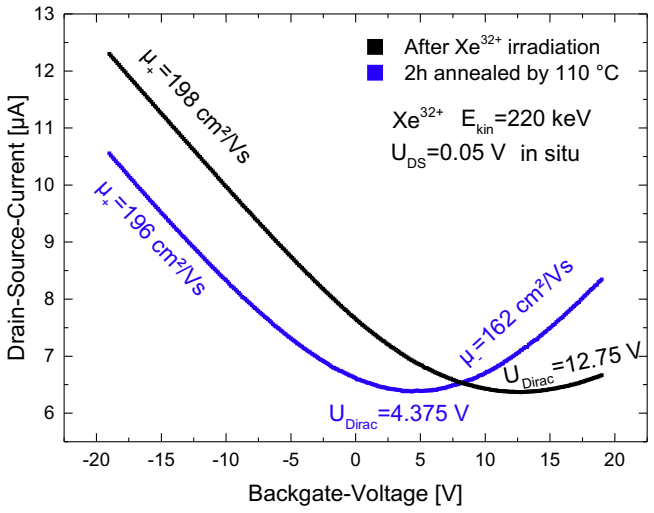

Fig. 5. Transfer characteristic (black) following $^{129}Xe^{32+}$-ion irradiation. After irradiation, the sample was annealed for 2 h at 110 °C (blue) and shows no noticeable differences in the hole mobility μ_+. But the Dirac point shifted to lower backgate voltages which indicates a n-doping. (For interpretation of the references to colour in this figure legend, the reader is referred to the web version of this article.)

Furthermore, by analyzing relative values, we present a method to eliminate the uncertainty with respect to the individual quality of a given G-FET.

The transfer characteristic $I_{DS}(U_{GS})$ measurements show, that HCIs do modify the electrical properties of graphene. In comparison with previous experiments with graphene irradiated by swift heavy ions (SHI) we observe a clearly different behavior. When graphene is irradiated with SHI, at low fluences an **increase** in charge carrier mobility has been observed [43], while for HCI we definitely observe a **decrease**. Both types of projectiles interact predominantly with the electronic system of the target and it has therefore been proposed, that the mechanism of defect creation might be similar [8]. However, when interacting with graphene, we need to consider the difference in energy deposition between the two projectiles. Highly charged ions typically dissipate almost all their potential energy in the surface [44]. In contrast, due to their large kinetic energy in the range of up to several MeV per atomic mass unit, SHI will penetrate not only the graphene layer, but will reach deep into the bulk material for some ten microns or more. The intense energy deposition into the electronic system of the bulk material will at one point be transferred to the lattice and may lead to a so-called thermal spike [45,46]. This localized heating of the substrate could lead to a local annealing of graphene [47] which would be absent in HCI irradiation.

Our data shows a clear dependence of the mobility reduction on the charge state, i.e. a projectile with a higher charge state is more efficient than an ion with a lower charge state. This is in agreement with previous results where it could be shown that size of the defective region is directly related to the potential energy of the HCI [17]. These defective regions are typically a few nm^2 in size. Future systematic experiments with G-FETs will reveal if and how the size of defect regions scales with the change of the transport properties. In particular, it would be interesting to determine the threshold charge state for the mobility reduction to be effective.

Acknowledgement

We thank the DFG for financial support within the framework of the SPP 1459 Graphene. We thank Dr.-Ing. Artur Poloczek and Dipl.Ing Gregor Keller at the HLT, Duisburg for sample preparation.

References

[1] J. Kopniczky, C.T. Reimann, A. Hallen, B.U.R. Sundqvist, P. Tengvall, R. Erlandsson, Scanning-force-microscopy study of MeV-atomic-ion-induced surface tracks in organic crystals, Phys. Rev. B 49 (1) (1993) 625–628.
[2] G. Hayderer, S. Cernusca, M. Schmid, P. Varga, H.P. Winter, F. Aumayr, STM studies of HCI-induced surface damage on highly oriented pyrolytic graphite, Phys. Scr. T92 (2001) 159.
[3] E. Akcöltekin, T. Peters, R. Meyer, A. Duvenbeck, M. Klusmann, I. Monnet, H. Lebius, S. Schleberger, Creation of multiple nanodots by single ions, Nat. Nanotechnol. 2 (2007) 290–294.
[4] A.S. El-Said, W. Meissl, M.C. Simon, J.R. Crespo Lopez-Urrutia, I.C. Gebeshuber, M. Lang, H.P. Winter, J. Ullrich, F. Aumayr, Surface nanostructures induced by slow highly charged ions on CaF_2 single crystals, Nucl. Instr. Meth. Phys. Res. B 256 (1) (2007) 346–349.
[5] T. Masahide, F. Yuso, Y. Chikashi, O. Shunsuke, Electronic interaction of individual slow highly charged ions with TiO_2(110), Phys. Rev. B 77 (15) (2008). 15427 1–4.
[6] R. Heller, S. Facsko, R. Wilhelm, W. Möller, Defect mediated desorption of the KBr(001) surface induced by single highly charged ion impact, Phys. Rev. Lett. 101 (9) (2008).
[7] S. Akcöltekin, S. Akcöltekin, T. Roll, H. Lebius, S. Schleberger, Patterning of insulating surfaces by electronic excitation, Nucl. Instr. Meth. Phys. Res. B 267 (8–9) (2009) 1386–1389.
[8] F. Aumayr, S. Facsko, A.S. El-Said, C. Trautmann, M. Schleberger, Single ion induced surface nanostructures: a comparison between slow highly charged and swift heavy ions, J. Phys. Condens. Matter 23 (39) (2011) 393001.

[9] R. Ritter, Q. Shen, R.A. Wilhelm, R. Heller, R. Ginzel, J.R. Crespo López-Urrutia, S. Facsko, C. Teichert, F. Aumayr, Novel aspects on the irradiation of HOPG surfaces with slow highly charged ions, Nucl. Instr. Meth. Phys. Res. B 315 (2013) 252–256.
[10] M. Karlusic, R. Kozubek, H. Lebius, B. Ban-d'Etat, R. Wilhelm, M. Buljan, Z. Siketic, F. Scholz, T. Meisch, M. Jaksic, S. Bernstoff, M. Schleberger, B. Santic, Response of GaN to energetic ion irradiation: conditions for ion track formation, J. Phys. D Appl. Phys. 48 (2015) 325304.
[11] O. Ochedowski, O. Osmani, M. Schade, B.K. Bussmann, B. Ban-d'Etat, H. Lebius, M. Schleberger, Graphitic nanostripes in silicon carbide surfaces created by swift heavy ion irradiation, Nat. Commun. 5 (2014) 3913.
[12] S. Akcöltekin, H. Bukowska, T. Peters, O. Osmani, I. Monnet, I. Alzaher, B. Ban-d'Etat, H. Lebius, S. Schleberger, Unzipping and folding of graphene by swift heavy ions, Appl. Phys. Lett. 98 (2011) 103103.
[13] O. Ochedowski, B. Kleine Bussmann, B. Ban-d'Etat, H. Lebius, S. Schleberger, Manipulation of the graphene surface potential by ion irradiation, Appl. Phys. Lett. 102 (2013) 153103.
[14] O. Ochedowski, S. Akcöltekin, B. Ban-d'Etat, H. Lebius, M. Schleberger, Detecting swift heavy ion irradiation effects with graphene, Nucl. Instr. Meth. Phys. Res. B 314 (2013) 18–20.
[15] O. Ochedowski, H. Bukowska, V.M. Freire Soler, L. Brökers, B. Ban-d'Etat, H. Lebius, M. Schleberger, Folding two dimensional crystals by swift heavy ion irradiation, Nucl. Instr. Meth. Phys. Res. B 340 (2014).
[16] R. Kozubek, O. Ochedowski, I. Zagoranskiy, M. Karlusic, M. Schleberger, Application of HOPG and CVD graphene as ion beam detectors, Nucl. Instr. Meth. Phys. Res. B 340 (2014).
[17] J. Hopster, R. Kozubek, B. d'EtatB, S. Guillous, H. Lebius, M. Schleberger, Damage in graphene due to electronic excitation induced by highly charged ions, 2D Mater. 1 (1) (2014) 011011.
[18] R. Wilhelm, E. Gruber, R. Ritter, R. Heller, S. Facsko, F. Aumayr, Charge exchange and energy loss of slow highly charged ions in 1 nm thick carbon nanomembranes, Phys. Rev. Lett. 112 (2014) 153201.
[19] O. Ochedowski, O. Lethinen, U. Kaiser, A. Turchanin, B. Ban-d'Etat, H. Lebius, M. Karlusic, M. Jakisic, M. Schleberger, Nanostructuring graphene by dense electronic excitation, Nanotechnology 26 (2015) 465302.
[20] A. Arnau, F. Aumayr, P.M. Echenique, M. Grether, W. Heiland, J. Limburg, R. Morgenstern, P. Roncin, S. Schippers, R. Schuch, N. Stolterfoht, P. Varga, T. Zouros, H.P. Winter, Interaction of slow multicharged ions with solid surfaces, Surf. Sci. Rep 27 (4–6) (1997) 113–239.
[21] J. Hopster, R. Kozubek, J. Krämer, V. Sokolovsky, M. Schleberger, Ultra-thin MoS_2 irradiated with highly charged ions, Nucl. Instr. Meth. Phys. Res. B 317 (2013) 165–169.
[22] F. Burgdörfer, F. Meyer, Image acceleration of multiply charged ions by metallic surfaces, Phys. Rev. A 47 (1) (1993) R20–R22.
[23] A.C. Ferrari, J.C. Meyer, V. Scardaci, C. Casiraghi, M. Lazzeri, F. Mauri, S. Piscanec, D. Jiang, K.S. Novoselov, S. Roth, A.K. Geim, Raman spectrum of graphene and graphene layers, Phys. Rev. Lett. 97 (18) (2006). 187401-187401.
[24] A.C. Ferrari, Raman spectroscopy of graphene and graphite: Disorder, electron–phonon coupling, doping and nonadiabatic effects, Solid State Commun. 143 (1–2) (2007) 47–57.
[25] A.C. Ferrari, D.M. Basko, Raman spectroscopy as a versatile tool for studying the properties of graphene, Nat. Nanotechnol. 8 (4) (2013) 235–246.
[26] K.S. Novoselov, Electric field effect in atomically thin carbon films, Science 306 (5696) (2004) 666–669.
[27] F. Schwierz, Graphene transistors, Nat. Nanotechnol. 5 (7) (2010) 487–496.
[28] B. Radisavljevic, A. Radenovic, J. Brivio, V. Giacometti, A. Kis, Single-layer MoS_2 transistors, Nat. Nanotechnol. 6 (3) (2011) 147–150.
[29] Y.-W. Tan, Y. Zhang, K. Bolotin, Y. Zhao, S. Adam, E.H. Hwang, S. Das Sarma, H.L. Stormer, P. Kim, Measurement of scattering rate and minimum conductivity in graphene, Phys. Rev. Lett. 99 (24) (2007). 246803–1 — 246803–4.
[30] Y.-C. Lin, C.-C. Lu, C.-H. Yeh, C. Jin, K. Suenaga, P.-W. Chiu, Graphene annealing: how clean can it be?, Nano Lett 12 (1) (2012) 414–419.
[31] Z. Cheng, O. Zhou, C. Wang, Q. Li, C. Wang, Y. Fang, Toward intrinsic graphene surfaces: a systematic study on thermal annealing and wet-chemical treatment of SiO_2-supported graphene devices, Nano Lett. 11 (2) (2011) 767–771.
[32] T. Peters, C. Haake, J. Hopster, V. Sokolovsky, A. Wucher, M. Schleberger, HICS: highly charged ion collisions with surfaces, Nucl. Instr. Meth. Phys. Res. B 267 (4) (2009) 687–690.
[33] M.M. Lucchese, F. Stavale, E.H. Martins Ferreira, C. Vilani, M. Moutinho, R.B. Capaz, C.A. Achete, A. Jorio, Quantifying ion-induced defects and Raman relaxation length in graphene, Carbon 48 (5) (2010) 1592–1597.
[34] L.G. Cançado, A. Jorio, E.H. Martins Ferreira, F. Stavale, C.A. Achete, R.B. Capaz, M.V.O. Moutinho, A. Lombardo, T.S. Kulmala, A.C. Ferrari, Quantifying defects in graphene via Raman spectroscopy at different excitation energies, Nano Lett. 11 (8) (2011) 3190–3196, http://dx.doi.org/10.1021/nl201432g.
[35] B.S. Elman, M.S. Dresselhaus, G. Dresselhaus, E.W. Maby, H. Mazurek, Raman scattering from ion-implanted graphite, Phys. Rev. B 24 (2) (1981) 1027–1034.
[36] G. Compagnini, F. Giannazzo, S. Sonde, V. Raineri, E. Rimini, Ion irradiation and defect formation in single layer graphene, Carbon 47 (14) (2009) 3201–3207.
[37] A. Gupta, G. Chen, P. Joshi, S. Tadigadapa, P. Eklund, Raman scattering from high-frequency phonons in supported n-graphene layer films, Nano Lett. 6 (12) (2006) 2667–2673.
[38] J. Maultzsch, S. Reich, C. Thomsen, Double-resonant Raman scattering in graphite: interference effects, selection rules, and phonon dispersion, Phys. Rev. B 70 (15) (2004).
[39] A. Eckmann, A. Felten, A. Mishchenko, L. Britnell, R. Krupke, K.S. Novoselov, C. Casiraghi, Probing the nature of defects in graphene by Raman spectroscopy, Nano Lett. 12 (8) (2012) 3925–3930.
[40] M. Dresselhaus, A. Jorio, M. Hoffman, G. Dresselhaus, R. Saito, Perspectives on carbon nanotubes and graphene Raman spectroscopy, Nano Lett. 10 (3) (2010).
[41] M. Bruna, A.K. Ott, M. Ijäs, D. Yoon, U. Sassi, A.C. Ferrari, Doping dependence of the Raman spectrum of defected graphene, ACS Nano 8 (7) (2014) 7432–7441.
[42] H.E. Romero, N. Shen, P. Joshi, H.R. Gutierrez, S.A. Tadigadapa, J.O. Sofo, P.C. Eklund, n-type behavior of graphene supported on Si/SiO_2 substrates, ACS Nano 2 (10) (2008) 2037–2044.
[43] O. Ochedowski, K. Marinov, G. Wilbs, G. Keller, N. Scheuschner, D. Severin, M. Bender, J. Maultzsch, F.J. Tegude, M. Schleberger, Radiation hardness of graphene and mos2 field effect devices against swift heavy ion irradiation, J. Appl. Phys. 113 (21) (2013) 214306.
[44] F. Aumayr, H. Winter, Potential sputtering, Phil. Trans. R. Soc. A 362 (1814) (2004) 77–102.
[45] M. Toulemonde, C. Dufour, E. Paumier, Transient thermal process after a high-energy heavy-ion irradiation of amorphous metals and semiconductors, Phys. Rev. B 46 (22) (1992) 14362–14369.
[46] M. Toulemonde, W. Assmann, A. Dufour, A. Meftah, C. Trautmann, Nanometric transformation of the matter by short and intense electronic excitation: experimental data versus inelastic thermal spike model, Nucl. Instr. Meth. Phys. Res. B 277 (2012) 28–39.
[47] S. Kumar, A. Tripathi, F. Singh, S. Khan, V. Baranwal, D. Kumar Avasthi, Purification/annealing of graphene with 100-MeV Ag ion irradiation, Nanoscale Res. Lett. 9 (126) (2014).